Doubly-Fed Induction Machine Models for Stability Assessment of Wind Farms

Markus A. Pöller

***Abstract*—The increasing size of wind farms requires power system stability analysis including dynamic models of the wind power generation. Nowadays, the most widely used generator type for units above 1MW is the doubly-fed induction machine. Doubly-fed induction machines allow active and reactive power control through a rotor-side converter, while the stator is directly connected to the grid. Detailed models for doubly-fed induction machines are well known but the efficient simulation of entire power systems with hundreds of generators requires reduced order models. This paper presents a fundamental frequency doubly-fed induction machine model including a typical control system and discusses the accuracy of reduced order models under various operating conditions.**

***Index Terms*— doubly-fed induction machines, off-shore wind power generation, power system stability, wind power generation, variable speed drives**

I. Introduction

THE totally installed wind power capacity is constantly increasing. End of June 2002, there were wind turbines with a total rated power of 9837,27 MW installed in Germany [1]. Not only the overall installed wind power capacity, but also the average rated power per wind mill is constantly increasing. In Germany, during the first six months of 2002, the average rated power per wind turbine went up to 1314 kW, which is an increase of 8% compared to the same period in 2001 [1].

Especially for wind mills above 2,0 MW, the doubly-fed induction generator is the most widely used generator concept (e.g. GE Wind Energy, Vestas, RE Power, Nordex, NEG Micon).

These figures clearly show that there is a strong need for power system stability analysis, including dynamic models of on- and off-shore wind farms. For dynamic power system analysis, different models, from fully detailed to highly reduced order models are proposed in the literature (e.g [5],[4]), but standard doubly- fed induction machine models for modeling large power systems are still under investigation [2].

This paper presents an approach for standard doubly-fed induction machine models for stability analysis. It includes models of all components, the induction generator, the rotor-side- and the grid-side converters and typical approaches for the control circuits and aerodynamics of the wind turbine.

All models have been implemented and tested in the power system analysis program DIgSILENT *PowerFactory* [10].

II. The Doubly-Fed Induction Machine Concept

Figure 1 shows the general concept of the doubly-fed induction generator. The mechanical power generated by the wind turbine is transformed into electrical power by an induction generator and is fed into the main grid through the stator and the rotor windings. The rotor winding is connected to the main grid by self commutated AC/DC converters allowing controlling the slip ring voltage of the induction machine in magnitude and phase angle.

Markus Pöller is with DIgSILENT GmbH, Heinrich-Hertz-Str. 9, 72810 Gomaringen, Germany (email: m.poller@digsilent.de)

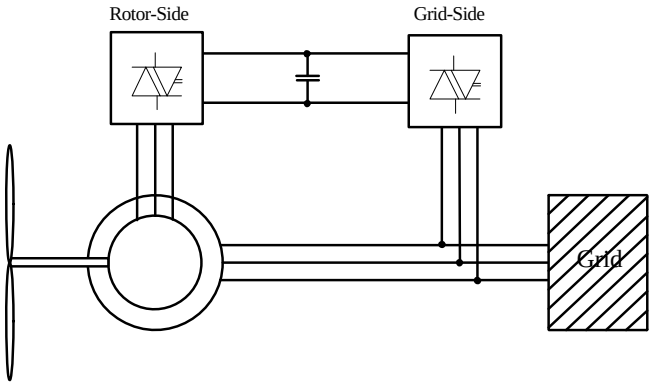

Fig. 1. Doubly-fed induction generator system

In contrast to a conventional, singly-fed induction generator, the electrical power of a doubly-fed induction machine is independent from the speed. Therefore, it is possible to realize a variable speed wind generator allowing adjusting the mechanical speed to the wind speed and hence operating the turbine at the aerodynamically optimal point for a certain wind speed range.

III. Induction Generator

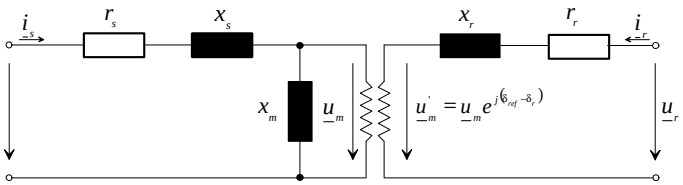

Fig. 2. Equivalent circuit of the doubly-fed induction generator

Fig. 2 shows the equivalent circuit diagram of the doubly-fed induction generator from which the model equations in a constantly, with ω_{ref} rotating reference frame can be derived as follows:

$$\underline{u}_s = r_s \underline{i}_s + \frac{d\underline{\psi}_s}{\omega_n dt} + j\frac{\omega_{ref}}{\omega_n}\underline{\psi}_s \quad (1)$$

$$\underline{u}_r = r_r \underline{i}_r + \frac{d\underline{\psi}_r}{\omega_n dt} + j\frac{\omega_{ref}-\omega_g}{\omega_n}\underline{\psi}_r \quad (2)$$

The flux linkage can be expressed by the following equations:

$$\underline{\psi}_s = (x_s + x_m)\underline{i}_s + x_m \underline{i}_r \quad (3)$$

$$\underline{\psi}_r = x_m \underline{i}_s + (x_m + x_r)\underline{i}_r \quad (4)$$

The induction machine model is completed by the mechanical equation:

$$J\frac{d\omega_g}{dt} = t_m + t_{el} \quad (5)$$

The electrical torque is calculated from the stator current and the stator flux:

$$t_{el} = \mathrm{Im}(\underline{\psi}_s \underline{i}_s^*) \tag{6}$$

All quantities are expressed in a stator-side per unit system.

This induction machine model of fifth order is able to represent rotor and stator transients correctly. In stability studies however, transient phenomena of the electrical network are usually not considered [7]. Applying the principle of neglecting stator transients to the doubly-fed induction machine model leads to the following third order model:

$$\underline{u}_s = r_s \underline{i}_s + j \frac{\omega_{ref}}{\omega_n} \underline{\psi}_s \tag{7}$$

$$\underline{u}_r = r_r \underline{i}_r + \frac{d\underline{\psi}_r}{\omega_n dt} + j \frac{\omega_{ref} - \omega_g}{\omega_n} \underline{\psi}_r \tag{8}$$

The mechanical equation is the same as in case of the fifth order model.

Neglecting rotor transients results in a first order induction machine model that consists of steady-state stator and rotor voltage equations.

$$\underline{u}_s = r_s \underline{i}_s + j \frac{\omega_{ref}}{\omega_n} \underline{\psi}_s \tag{9}$$

$$\underline{u}_r = r_r \underline{i}_r + j \frac{\omega_{ref} - \omega_g}{\omega_n} \underline{\psi}_r \tag{10}$$

The only dynamic equation of the first order model is the mechanical equation according to (5).

A. Rotor Current Protection

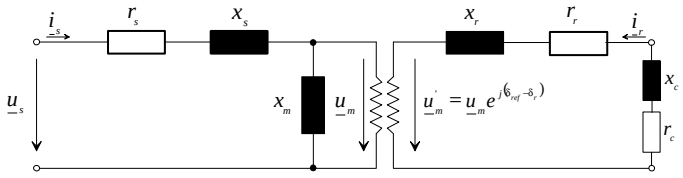

Fig. 3. Doubly-fed induction generator with inserted crow-bar protection (r_c and x_c

In case of faults near to the generator, rotor currents are increasing and risk to damage the rotor-side converter. For avoiding any damages, the rotor-side converter is bypassed when the rotor currents exceed a certain limit ("crow-bar" protection, see Fig. 3).

While the rotor-side converter is bypassed, the generator operates as a normal induction generator. Since the speed can be considerably above synchronous speed before a fault occurs or the machine quickly accelerates during a fault, the stalling point of the machine is usually exceeded during a fault leading to very high reactive power consumption. Bypassing the rotor with an additional resistance and an additional reactance (see r_c and x_c in Fig. 3) shifts the stalling point to a higher speed value and reduces the machine's reactive power consumption considerably . This mode of operation can be considered in the rotor-voltage (2) and the rotor flux-linkage equation (4) as follows:

$$\underline{0} = (r_r + r_c)\underline{i}_r + \frac{d\underline{\psi}_r}{\omega_n dt} + j \frac{\omega_{ref} - \omega_g}{\omega_n} \underline{\psi}_r \tag{11}$$

$$\underline{\psi}_r = x_m \underline{i}_s + (x_m + x_r + x_c)\underline{i}_r \tag{12}$$

The crow-bar protection is usually removed after a pre-defined time. Additional criteria, such as voltage magnitude, can be considered for increasing the reliability of the rotor current protection system.

In the DIgSILENT *PowerFactory* implementation, the crow-bar protection is integral part of the doubly-fed induction machine model. Criteria for inserting and removing the rotor-bypass can be flexibly defined using *PowerFactory*'s simulation language.

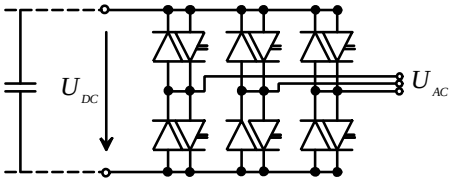

Fig. 4. VSC-PWM converter

IV. Rotor- and Grid-Side Converters

The rotor- and grid-side converters are self-commutated converters and are usually set-up by six-pulse bridges according to Fig. 4.

Assuming an ideal DC-voltage and an ideal PWM modulation (infinite modulation frequency), the fundamental frequency line to line AC voltage (RMS value) and the DC voltage can be related to each other as follows:

$$|U_{AC}| = \frac{\sqrt{3}}{2\sqrt{2}} P_m U_{DC} \tag{13}$$

The AC-voltage phase angle is defined by the PWM converter.

The pulse-width modulation factor P_m is the control variable of the PWM converter. Equation (13) is valid for $0 <= P_m < 1$. For values larger than 1 the converter starts saturating and the level of low order harmonics starts increasing. The complete characteristic of the PWM converter, including the saturated range is shown in Fig. 5.

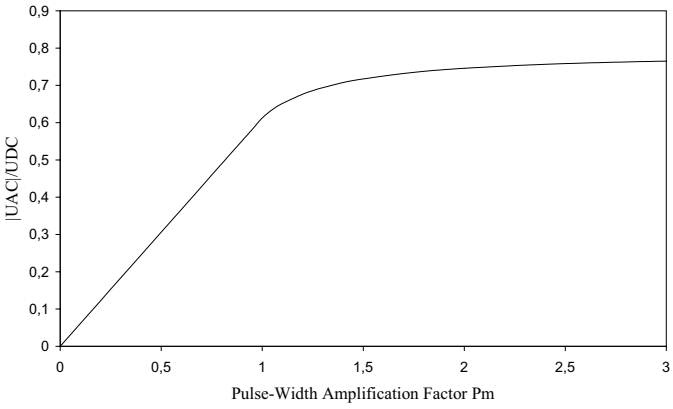

Fig. 5. PWM Converter fundamental frequency characteristic

The converter model is completed by the power conservation equation:

$$U_{DC} I_{DC} + \sqrt{3}\mathrm{Re}\,(\underline{U}_{AC} \underline{I}_{AC}^*) = 0 \tag{14}$$

This equation assumes a loss-less converter. Because the switching frequency of PWM converters is usually very high (typically several hundreds Hz), switching losses are the predominant type of losses. Since the average switching losses are basically proportional to U_{DC}^2, switching losses can be considered by a resistance between the two DC-poles in a fundamental frequency model.

V. Control Concept

Amongst the big variety of different control concepts for variable speed wind turbines (e.g. [4], [6]) a typical concept consisting of dq-current regulators for the generator control and a maximum power tracking strategy for the wind turbine control is presented and analyzed in this paper.

A. Rotor-Side Converter

The rotor-side converter operates in a stator-flux dq-reference frame that decomposes the rotor current into an active power (q-axis) and a reactive power (d-axis) component.

A very fast inner control loop regulates the active- and the reactive component of the rotor current. The current-setpoints are defined by a slower outer control loop regulating active and reactive power (see Fig. 6).

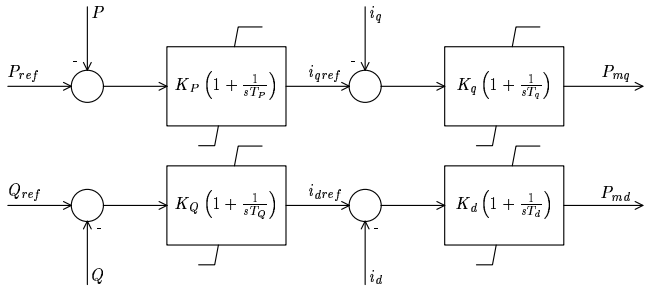

Fig. 6. Rotor-side converter controller

B. Grid-Side Converter

The control concept of the grid-side converter is very similar to the rotor-side controller concept. The grid-side converter controller operates in an AC-voltage dq-reference system. Active and reactive components of the grid-side converter currents are regulated by a fast inner control loop (see Fig. 7). A slower outer control loop defining the q-current setpoint regulates the DC-voltage to a pre-defined value. The setpoint of the d-axis component can be used for optimum reactive power sharing between the generator and the grid-side converter or simply kept to a constant value.

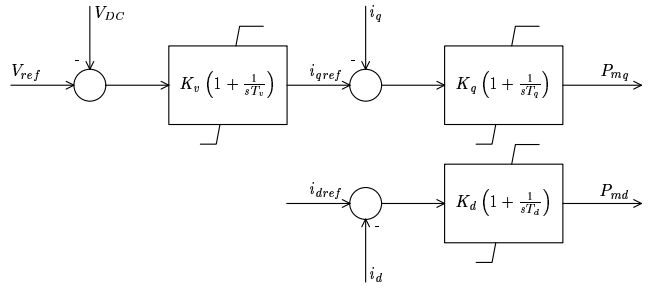

Fig. 7. Grid-side converter controller

C. Reactive Power Control

Reactive power control is possible through the d-axis component of the rotor- and the grid-side converters. Variable speed wind power generators can be operated at a constant power factor, which is the standard operation mode today. Alternatively, an AC-voltage controller defining the d-axis current setpoint can be used in Fig. 6 instead of the Q-controller, or secondary voltage control can be supported by adjusting the Q-reference value (e.g. [4]).

D. Reduced Order Converter Model

For longer term simulations, when calculation time becomes an important issue, it might be desirable to neglect the very fast time constants associated with the DC intermediate circuit shown in Fig. 4. When neglecting the DC-capacitance, the DC currents of the rotor- and grid-side converters are forced to be equal. Consequently, the grid-side controller must be replaced by an ideal voltage controller, without the inner current control loops. On the AC side, the active power injection is defined by the power conservation between AC and DC according to (14). For defining the reactive power balance, the d-axis current component (reactive current) of the grid-side converter can directly be set by a reactive power controller or a constant reactive current component can be assumed.

A further model reduction consists of completely neglecting the time constants of the DC voltage controller. The grid-side converter and it's controls is then modeled by a steady-state device, keeping the DC voltage constant. With this simplification however, saturation effects (see Fig. 5)in the grid-side controller cannot be considered.

E. Turbine Control

Equation (15) shows the aerodynamic equation of a wind turbine that relates mechanical power to wind speed and mechanical speed of the turbine (e.g. [5]):

$$P_t = \frac{\rho}{2}\pi R^2 c_p(\lambda, \beta) v_w^3 \tag{15}$$

with:
P_t: Mechanical power of the wind turbine
ρ: Air density
R: Rotor radius
λ: Tip speed ratio
β: Blade pitch angle
c_p: Power coefficient as a function λ and β
v_w: Wind speed

The tip speed ratio λ is defined as follows:

$$\lambda = \frac{\omega_t R}{v_w} \tag{16}$$

with ω_t being the mechanical frequency of the wind turbine.

Equation (15) defines the steady-state aerodynamic behaviour of a wind turbine; it cannot reflect dynamic stall effects correctly. An approximate method for including dynamic stall effects is described in [9].

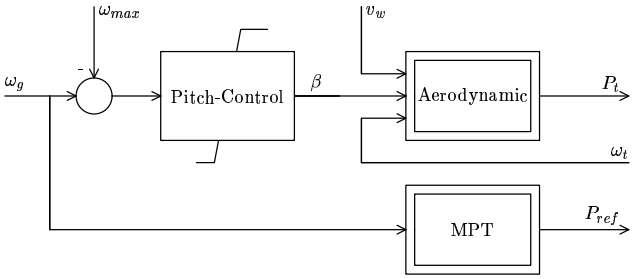

Fig. 8. Generic wind turbine model

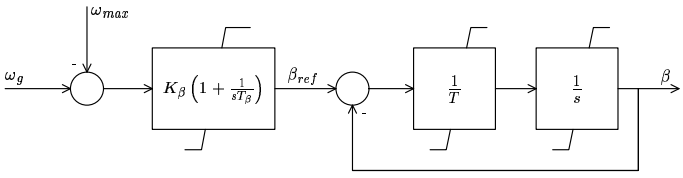

Fig. 9. Generic model of the pitch-control system

A generic wind turbine model for stability studies based on a maximum power tracking strategy [5] can be implemented according to Fig. 8.

In case of rotor frequencies below ω_{max}, active power is regulated according to the maximum power tracking (MPT) characteristic that defines the maximum power depending on the shaft speed as power reference of the power controller. When the maximum shaft speed is reached, the active power setpoint remains constant and the pitch angle control system (see Fig. 9) starts acting driving the shaft speed back to the maximum permitted value.

An alternative control scheme is described in [4]. Here, the speed reference is calculated from the actually generated electrical power (inverse MPT characteristic). As a result, the generator is driven into optimal speed. When P_{max} is reached, the pitch angle control takes over and regulates the actual power to P_{max}.

F. Wind Fluctuations

Wind fluctuations can be modeled by varying the wind-speed-input v_w of the aerodynamic block in Fig. 8.

Wind speed is usually modeled by superposing several deterministic and stochastic components. However, since the response of doubly-fed induction machines to system faults is in the center of interest of this paper and wind speed can be assumed to be constant in these cases, no concrete wind-speed models are described here. Generally, common wind-speed models (e.g. [9]) can be combined with the models presented in this paper.

G. Torsional Oscillations

When the simulated applications are limited to the impact of wind fluctuations, it is usually sufficient to consider just a single-mass shaft model because shaft oscillations of variable speed wind generators are not reflected to the electrical grid due to the fast active power control. [5].

In stability analysis however, when the system response to heavy disturbances is analyzed, the shaft must be approximated by at least a two mass model. One mass represents the turbine inertia, the other mass is equivalent to the generator inertia.

The equations describing the mechanical coupling of turbine and generator through the gear box by a two-mass model can be expressed as follows (see e.g. [8]):

$$J_t \frac{d\tilde{\omega_t}}{dt} = t_t - t_m \tag{17}$$

$$J_g \frac{d\omega_g}{dt} = t_m + t_{el} \tag{18}$$

$$\frac{d\Theta_{tg}}{dt} = \tilde{\omega_t} - \omega_g \tag{19}$$

$$t_m = K_{tg}\Theta_{tg} + D_{tg}(\tilde{\omega_t} - \omega_g) \tag{20}$$

In these equations turbine inertia, turbine torque and turbine frequency $\tilde{\omega_t}$ are related to the generator nominal frequency. The turbine torque is related to the turbine power (see Fig. 8) by:

$$t_t = \frac{P_t}{\tilde{\omega_t}}$$

The electrical torque is defined by (6).

VI. Case Studies

For validating the presented models, the results of simulating a heavy and a relatively weak disturbance in the system shown in Fig. 10 are described.

The system consists of an external infeed modeled by a source behind an impedance that is connected to a synchronous generator through a line. And wind farm consisting of three doubly-fed induction generators with a rating of 5MW each is connected to the mid-point of the transmission line.

Each doubly-fed induction generator is modeled according to Fig. 11, including the three winding transformer, the induction generator, the grid-side and the rotor-side converter and the intermediate DC-circuit.

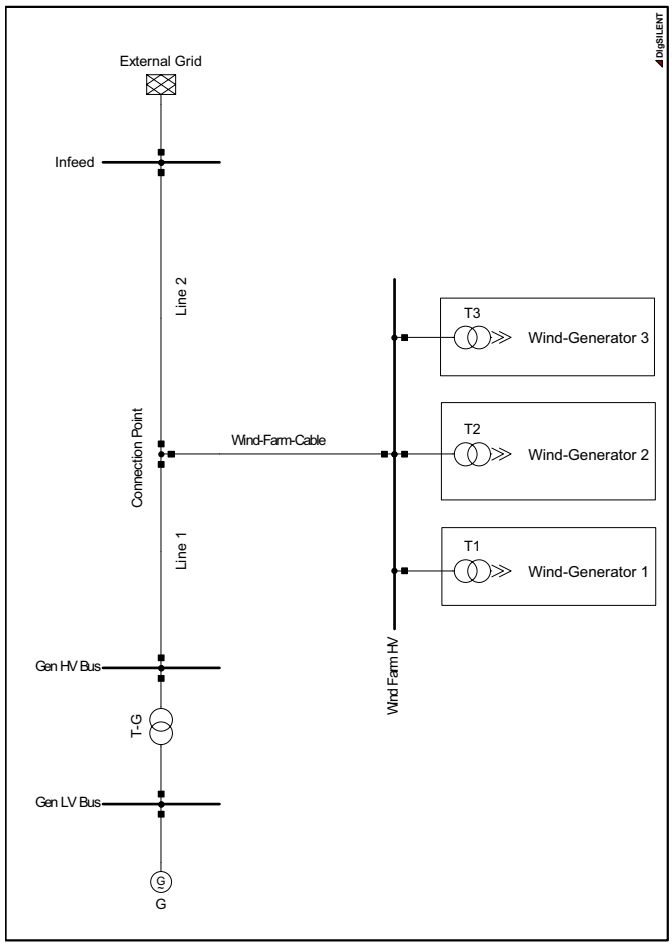

Fig. 10. Power system used for model validation

A. Strong Disturbance

The first case simulates a solid three phase short circuit (duration: 200ms) at the "Connection Point" (see Fig. 11). The rotor-current-protection systems bypass the rotor-side converters immediately after the fault has been inserted (see Fig. 12 and Fig. 13). After the fault was cleared, at t=200ms, the generators continue to operate with bypassed converters until t=800ms, when the "crow-bars" are removed. When the converters are back into operation, the system is driven back to the initial state.

The speed shows a weakly damped torsional oscillation.

Fig. 12 compares the results obtained with a fifth order induction generator model according to (1) and a third order model according to (7).

In the simulation of the fifth order model, not only stator transients of the induction machine but also the transient behaviour of transformers and lines was considered (EMT-compatible network model).

Together with the third order machine model, a quasi-steady-state network model was used, corresponding to the classical "stability"-approach as described e.g. in [7].

When comparing the results from both models, as shown in Fig. 12, it can be noted that the reduced order model represents the average of power and voltage very well. Higher frequency transients, as they can be observed in the results from the detailed model, are due to network transients and are therefore not represented by the reduced order model. The reduced order model can therefore be used for analyzing the influence of doubly-fed induction machines to the power system, but it is not possible to predict peaks in electrical power or torque correctly. Therefore, the fifth order model together with a "transient" network model is required.

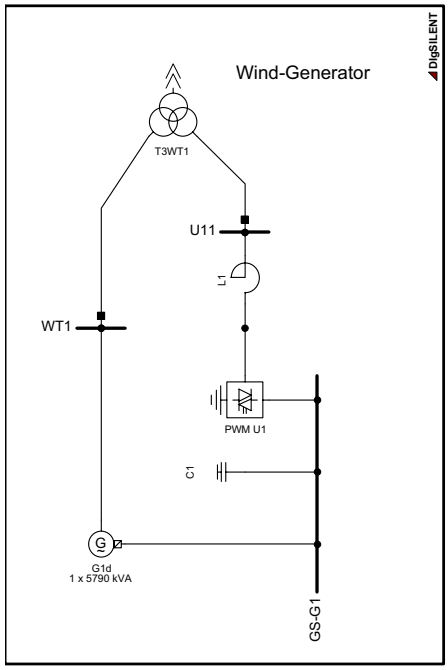

Fig. 11. Wind Generator with detailed grid-side converter

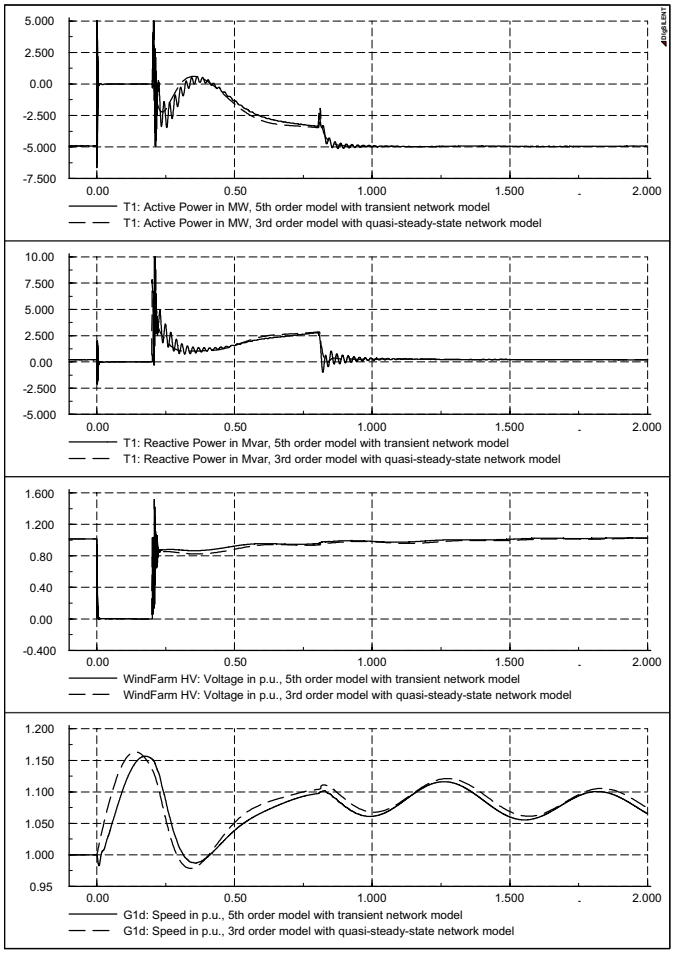

Fig. 12. Comparison of fifth order and third order model in case of a three phase fault near to the wind generators

The ”speed” variable highlights differences between the two models: In the detailed model, the speed is initially reduced before the system starts accelerating. In the reduced order model however, the machine starts accelerating immediately after the fault was inserted.

The initial speed reduction, as shown by the detailed model, is a consequence of decaying DC-components in the machine’s currents and is known as the ”back-swing” effect of electrical machines. Since the third order model does not represent stator transients, the initial back-swing is not represented by the reduced order model leading to an immediate acceleration.

Fig. 13 compares the results of further model reductions:

1) Third order model with detailed grid-side converter, the same as in Fig. 12
2) Third order model with simplified grid-side converter, as described in section V-D (complete reduction of the intermediate DC-circuit.)
3) First order model with simplified grid-side converter.

All results are in good agreement. Especially the reduction of the grid-side converter does not seem to have a big impact on the model accuracy when system stability is studied. The first order model however does not represent any rotor flux transients and differs therefore from the other curves during a short period after a heavy disturbance.

With regard to computational efficiency, some information about the integration step-size might be of interest. All models were implemented and tested in DIgSILENT *PowerFactory* [10]. *PowerFactory* uses a variable step size algorithm, in which the minimum step size can be specified by the user. During the simulation, the step size is automatically increased whenever the accuracy of the numerical algorithm allows for it.

In case of the fully detailed, fifth order machine model in combination with a transient network model (Fig. 12), the step size varied between $0,1$ms and 2ms. In case of the reduced order models together with the steady-state network model it varied between 1ms and 50ms. The calculation time of the third order and first order model was practically the same.

B. Weak Disturbance

In a second case, a three phase short circuit at the synchronous generator terminal was simulated (”Gen-LV-Bus”). This short circuit causes the voltage at the wind park terminal to drop to about 0.6 p.u. (see Fig. 14). Because the rotor current protection is not triggered, the disturbance can be classified as a fault remote from the wind park.

As Fig. 14 shows, the three wind turbines are differently loaded in this case.

While the fault is in the system, the active and reactive power controllers remain in operation why active and reactive power is fully controlled.

Clearing the fault disturbs the system again, but active and reactive power are well regulated. The speed of all turbines shows a weakly damped torsional oscillation.

These simulations were carried out with the third order model and the simplified grid-side converter model. The model represents very well the initial active and reactive power transients and the controller response following to the disturbance.

VII. Conclusions

This paper presented a variable speed wind generator model suited for stability analysis of large power systems with large on-shore and off-shore wind farms. The presented components were the doubly-fed induction generator, the grid-side converter, the rotor-side converter, the aerodynamic behaviour of the wind turbine and the pitch control system.

For simulating power fluctuations, the wind speed variable must be fed from a measurement file, or stochastic wind models must be used (e.g. [9]).

Possible model reductions making the model suitable for stability assessment in large power systems were presented and discussed.

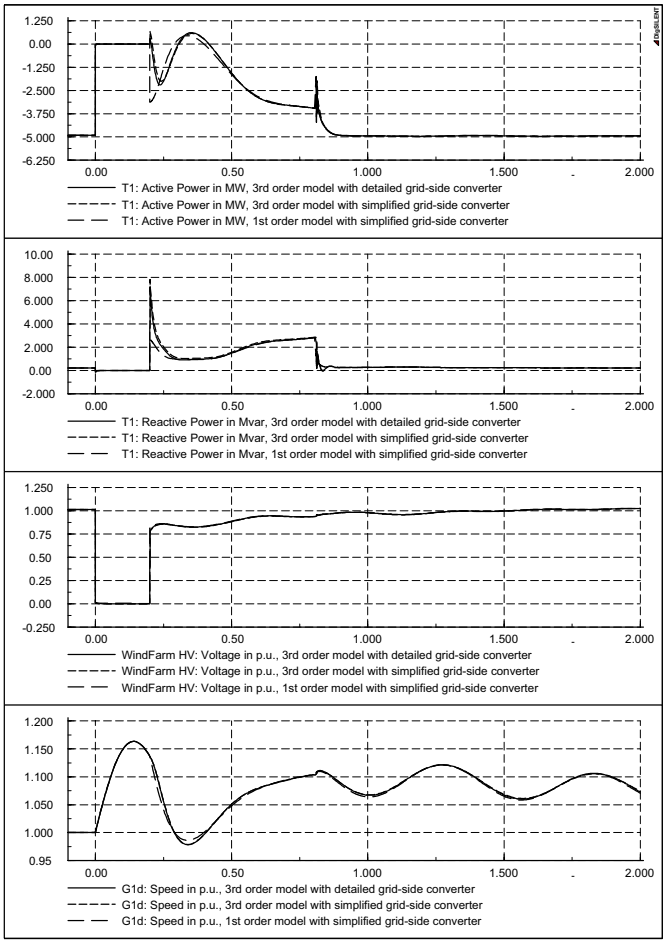

Fig. 13. Comparison of models of various order in case of a three phase fault near to the wind generators

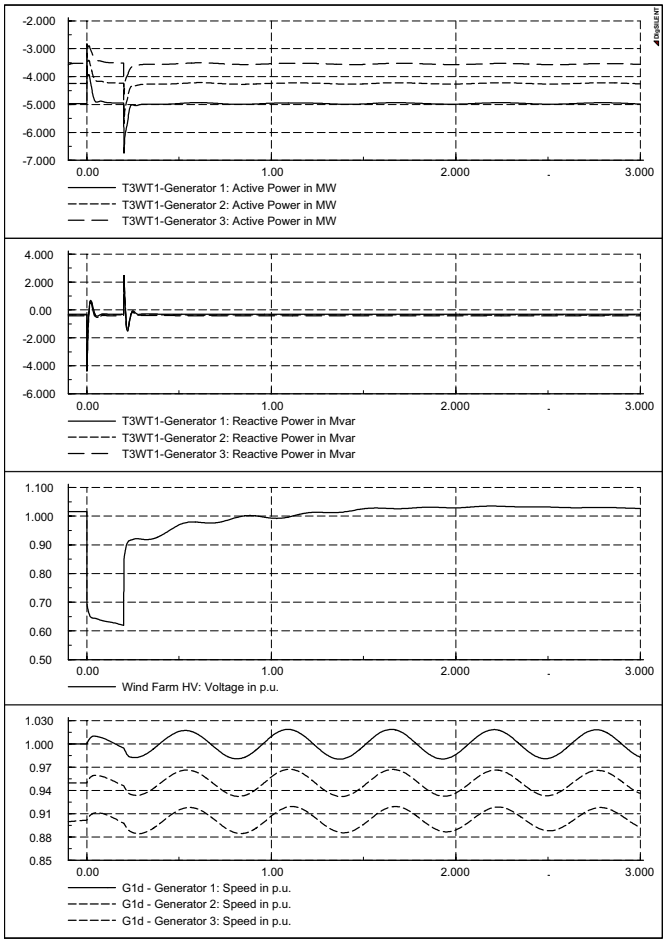

Fig. 14. Simulation of a weak disturbance (without crow-bar insertion)

The models were implemented and tested in the power system analysis package DIgSILENT *PowerFactory* [10]. Every reduced order model was validated against higher order models.

The results of the test cases show that a third order induction machine model including crow bar protection together with a simplified model of the grid-side converter provides sufficient accuracy and the necessary computational efficiency for carrying out stability studies in large power systems with several hundreds of machines.

REFERENCES

[1] C. Ender, "Wind Energy Use in Germany - Status 30.06.2002," *DEWI Magazin* Nr. 21, August 2002

[2] S. Stapelton and George Rizopoulos, "Dynamic Modelling of Modern Wind Turbine Generators and Stability Assessment of On- and Off-Shore Wind Farms " *Proceedings of the 3rd MED POWER Conference*, 2002

[3] C. R. Kelber and W. Schumacher, "Adjustable Speed Constant Frequency Energy Generation with Doubly-Fed Induction Machines" *Proceedings of the European Conference Variable Speed in Small Hydro, Grenoble, France*, 2000

[4] J. L. Rodriguez-Amenedo, "Automatic Generation Control of a Wind Farm With Variable Speed Wind Turbines," *IEEE Transactions on Energy Conversion*, Vol 17, No. 2, June 2002

[5] J. G. Slootweg, S. W. H. de Haan, H. Polinder, W. L. Kling, "Aggregated Modelling of Wind Parks with Variable Speed Wind Turbines in Power System Dynamics Simulations," *Proceedings of the 14th Power Systems Computation Conference*, Sevilla, 2002

[6] W. Hofmann and F. Okafor "Doubly-Fed Full-Controlled Induction Wind Generator for Optimal Power Utilisation," *Proceedings of the PEDS'01*, 2001

[7] P. Kundur "Power System Stability and Control," *McGraw-Hill, Inc.*, 1994

[8] P. M. Anderson, B. L. Van Agrawal and J. E. Ness, "Subsynchronous Resonance in Power Systems," *IEEE Press, New York*, 1989

[9] P. Soerensen, A.D. Hansen, L. Janosi, J. Bech and B. Bak-Jensen "Simulation of interaction between wind farm and power system", Technical-Report, *Risoe-R-128(EN)*, 2001, http://www.risoe.dk/rispubl/VEA/veapdf/ris-r-1281.pdf

[10] DIgSILENT GmbH "DIgSILENT *PowerFactory* V13 - User Manual," *DIgSILENT GmbH*, 2002

Markus Pöller was born in Stuttgart, Germany on July 22, 1968.
In 1995, he received Dipl.-Ing. degrees from the University of Stuttgart and Ecole Nationale Supérieure des Télécommunications Paris. In 2000, he received the Dr.-Ing. degree from the University of Hannover. Since 1995 he works with DIgSILENT GmbH, Germany, where he is responsible for the algorithms and models of the power system analysis software DIgSILENT *PowerFactory*. He is also involved in power system studies and he presents software- and power system analysis courses. His current research interests include wind power systems, optimal power flow dispatch and probabilistic load flow analysis.